PLOS ONE

RESEARCH ARTICLE

A new buffering theory of social support and psychological stress

Stelios Bekiros[1,2]*, **Hadi Jahanshahi**[3], **Jesus M. Munoz-Pacheco**[4]

1 LSE Health Centre & Department of Health Policy, London School of Economics and Political Science (LSE), London, United Kingdom, **2** Faculty of Economics &Management (FEMA), University of Malta, Msida, Malta, **3** Department of Mechanical Engineering, University of Manitoba, Winnipeg, Canada, **4** Faculty of Electronics Sciences, Benemerita Universidad Autonoma de Puebla, Puebla, Mexico

* S.Bekiros@lse.ac.uk, stelios.bekiros@um.edu.mt, stelios.bekiros@eui.eu

Citation: Bekiros S, Jahanshahi H, Munoz-Pacheco JM (2022) A new buffering theory of social support and psychological stress. PLoS ONE 17(10): e0275364. https://doi.org/10.1371/journal.pone.0275364

Editor: Mohammed S. Abdo, Hodeidah University, YEMEN

Received: March 10, 2022

Accepted: September 15, 2022

Published: October 12, 2022

Data Availability Statement: All relevant data are within the paper.

Funding: The authors received no specific funding for this work.

Competing interests: The authors have declared that no competing interests exist.

Abstract

A dynamical model linking stress, social support, and health has been recently proposed and numerically analyzed from a classical point of view of integer-order calculus. Although interesting observations have been obtained in this way, the present work conducts a fractional-order analysis of that model. Under a periodic forcing of an environmental stress variable, the perceived stress has been analyzed through bifurcation diagrams and two well-known metrics of entropy and complexity, such as spectral entropy and C0 complexity. The results obtained by numerical simulations have shown novel insights into how stress evolves with frequency and amplitude of the perturbation, as well as with initial conditions for the system variables. More precisely, it has been observed that stress can alternate between chaos, periodic oscillations, and stable behaviors as the fractional order varies. Moreover, the perturbation frequency has revealed a narrow interval for the chaotic oscillations, while its amplitude may present different values indicating a low sensitivity regarding chaos generation. Also, the perceived stress has been noted to be highly sensitive to initial conditions for the symptoms of stress-related ill-health and for the social support received from family and friends. This work opens new directions of research whereby fractional calculus might offer more insight into psychology, life sciences, mental disorders, and stress-free well-being.

1. Introduction

Stressful events are strongly connected to social factors [1]. Moreover, since the highly influential Cohen's study [2], social support and its interaction with stress have been tightly tied to factors affecting health and well-being. More precisely, social support received from family and friends has proven to positively impact health by moderating the adverse effects of stress. In fact, the more social support an individual receives, the better overall mental and physical health he or she will have [3, 4]. In this respect, some studies also suggest that social support affects mental health rather than physical health, and those diverse kinds of support can have different effects on perceived stress [5, 6].

So far, a variety of mathematical models have been used to understand and predict real-world phenomena [7–14]. Thus, finding a model accurately describing psychological dynamics could pave the way for long and short-term predictions of mental diseases, as well as for designing appropriate therapies [15]. In other words, mathematical modeling aims to anticipate the dynamics of psychological systems and control them as effectively as possible concomitant diseases. Some seminar studies dealing with the modelling of psychological phenomena can be found in [16, 17].

So far, a lot of research has been done on psychological stress [18–20]. In [21], the effects of long-lasting psychological stress on social behaviours is investigated using a predator stress model. In [22], Kapasia et al. attempt to examine factors associated with psychological stress as well as academic satisfaction and future academic risk during the COVID-19 epidemic. In another study, various stressors related to covid-19, including risk exposure, limited medical treatment access, reduced income, and perceived discrimination, and their association with psychological distress were investigated [23]. They found that social support in the neighborhood can reduce psychological distress and buffer the effects of stressors. This is while the support of family and friends has a limited effect on coping with stress. Stress-buffering hypothesis has been introduced to interpret the effect of stress moderation [24]. This hypothesis states that stress moderation may happen by processes associated with the value of social support (main effects), as well as by processes associated with the value of social support and stress (which is called buffering effect). In other words, buffering represents the interaction of the stressor levels with the social support received from friends and family. Thus, when the level of stress increases, the buffering effect becomes more critical. This stress moderation hypothesis has provided a fruitful situation for the advent of more complex models that investigate the relationships between stress, support, and illness. Hence, psychological models considering factors that are related to the buffering effect have attracted considerable attention in the last years [25, 26].

As a matter of fact, the development of trustable tools is the most critical challenge in the modeling of real-world, practical systems [27–31]. To reach this goal, fractional calculus has been recently proposed as a useful alternative [32, 33]. Indeed, fractional calculus is an excellent tool for the description of hereditary properties and memory of systems, which has been applied in a wide variety of scenarios in the last years [34–38]. Also, recently, the application of fractional calculus in social events and even disease dynamics have attracted a lot of attention. In [39–41] various fractional-order models of the transmission dynamics of COVID-19 have been proposed and studied.

In [42], a fractional-order dynamic model of love has been examined and its chaotic behaviour has been studied by investigating different orders. Additionally, in [43], the rich dynamics of a fractional-order love system with the fractional order derivative and model parameters have been studied. Furthermore, the control problem has been theoretically investigated. In [44], through fractional-order differential equations, dynamical model of happiness has been studied. By classifying persons of different personalities and impact factors of memory (IFM) with a distinct set of model parameters, it has been illustrated that such fractional-order models might display multiple behaviors with and without external situations. In [45], chaos control and dynamical synchronization model of happiness with fractional order have been studied.

Nonetheless, no study has used these fractional techniques to investigate the influence of social support buffering on stress. Despite the fact that fractional calculus gives a helpful and practical viewpoint in the modeling of real-world systems, publications that employ fractional calculus to describe psychological dynamics are rare. As a result, there is still an opportunity for improvement in nonlinear models that take into account the impacts of social support

buffering on physiological stress. Motivated by this, the current study introduces for the first time a fractional-order analysis of a previously published dynamic model of stress-related processes.

The suggested modelling, which provides a generalization dynamic of social support and psychological stress, is justified by the fact that the time evolution of psychological interactions, like other fractional systems, is inherently affected by memory. The fractional-order model is introduced, and its parameters are delineated. Then, in addition to bifurcation diagrams, analyses of entropy and complexity are also conducted in terms of spectral entropy and C_0 complexity. Considering a periodic variation in environmental stress, as well as a self-kindling in the subject's stress response, new and interesting insights into the relationships between stress, social support, and health are obtained. For instance, it is shown that stress experienced by an individual is strongly affected by initial conditions for physical or mental symptoms, as well as for the received social support.

The rest of the study is planned as follows. Section 2 describes the mathematical model of socially buffered stress processes and some basic concepts about fractional calculus. Afterward, the fractional-order model of the socially buffered stress processes is proposed as a new approach, and some of its properties are delineated. Section 3 outlines entropy and complexity analyses conducted on the resulting time series from the proposed approach. Finally, the main conclusions of the present study are summarized in Section 4.

2. Stress-buffering hypothesis

The socially buffered response model can be expressed as follows [46, 47]:

$$\frac{dX(t)}{dt} = k_1 A + (k_2 B - k_6)X(t) + k_3 Y(t) - k_4 X(t)Z(t) - k_5 X^2(t), \tag{1}$$

$$\frac{dY(t)}{dt} = k_6 X(t) - k_7 Y(t), \tag{2}$$

$$\frac{dZ(t)}{dt} = k_8 (S_0 - Z(t))Y(t) - \beta k_4 X(t)Z(t) - k_9 Z(t), \tag{3}$$

where $X(t)$ denotes the perceived psychological stress, including factors such as the person's cognitive appraisal [48], and the perceived psychological stress measured by observed stressors, self-reported, taxing life events, or hassles regarding an event [49]. The variable $Y(t)$ indicates the symptoms of stress-related ill-health, which can obtain through diverse clinical instruments. Moreover, $Z(t)$ stands for the received social support. This variable can be estimated via the received emotional and tangible assistance, the number of involved family members and friends, and so forth. In this model, it is also supposed that there exists bounded social support. Therefore, $S_0 = Z+U$, where Z and U respectively indicate the social support currently in use and the social support existing at the present time but not involved in buffering stress. Consequently, S_0 indicates the total available social support. The rate parameters k_i (*for* $i = 1,\ldots,9$) depend on the personality and features of the individual under stress. A and B respectively refer to the theoretical and experimental measures of environmental stress. More precisely, A indicates the environmental circumstances that directly cause a raising of the stress response, and B refers to the events and circumstances where the growth of stress happens due to the existence of stress itself. By fitting the model, all weights can be estimated for every particular individual and environment [46].

The model is quite similar to the one presented by Oregonator [50], which is a successful model of the oscillatory Belousov–Zhabotinsky chemical reaction. The matching of the model with real-world results has been clearly demonstrated by Epstein and Pojman [51]. Also, it has been shown that selecting suitable values for the described parameters results in psychologically reasonable outcomes, thus exhibiting oscillation, multiple stationary states, spatial pattern formation, bursting, and chaos [46]. Moreover, for most parameters, states of the system exhibit unchanging stationary values, suggesting that the model converges to "normal" dynamics of stress and symptoms of illness, and moreover, demonstrating recent interpretations of homeostasis [47].

Field and Schuldberg [47] have conducted a search of parameters on the presented model, which demonstrated that the model (Eqs (1)–(3)) does not show chaotic behavior in support seeking and stress levels. However, when the environmental stress value A changes periodically, chaos was detected for some conditions [46]. To this end, the following pattern for A was considered:

$$A = A_0 + \rho \sin(\omega t), \tag{4}$$

where ω and ρ denote the angular frequency and amplitude of the modulation, respectively. The magnitude and frequency of stress are two key factors that affect the system stability. Thus, when these parameters increase, the person experiences a more extensive and more rapid incidence of stressors. Also, high levels of stress over an extended period of time result in "complex trauma" [52]. In general terms, such conditions can bring new diagnostic categories and trauma disorders [53]. In what follows, we propose and investigate a pioneering fractional-order model of the socially buffered stress processes.

2.1. Fractional-order modeling

Fractional-order derivatives have been used widely, not only in an artificial way, but also with real-world physical phenomena [54]. They have been pointed out as valuable tools for understanding biological phenomena. In this way, a fractional form of the system described in Eqs (1)–(3) can be expressed as follows:

$${}_{t0}^{C}D_t^{q_1} X(t) = k_1 A + (k_2 B - k_6)X(t) + k_3 Y(t) - k_4 X(t)Z(t) - k_5 X^2(t), \tag{5}$$

$${}_{t0}^{C}D_t^{q_1} Y(t) = k_6 X(t) - k_7 Y(t), \tag{6}$$

$${}_{t0}^{C}D_t^{q_1} Z(t) = k_8 (S_0 - Z(t))Y(t) - \beta k_4 X(t)Z(t) - k_9 Z(t), \tag{7}$$

where $A = A_0 + \rho \sin(\omega t)$, and the values selected for the system parameters are listed in Table 1. These values were taken from [2].

It is well-known that fractional calculus is a generalization of differentiation and integration of non-integer order, defined by a continuous integro-differential operator ${}_{t0}^{C}D_t^{q_1}$, where α and t are the limits of the operation and $q \in \mathbb{R}$. In the literature, there are many definitions for the integro-differential operator. However, all are not adequate to define whether an operator can be considered as fractional. An excellent work published by Ortigueria et al. addresses this challenge by analyzing several definitions of fractional derivatives [55]. An operator is

Table 1. Values selected for the system parameters.

Parameter	A_0	S_0	β	k_1	k_2	k_3	k_4	k_5	k_6	k_7	k_8	k_9
Value	1	10	0.5	1	1	0.01	2	0.3	0.01	0.01	0.1	0.01

https://doi.org/10.1371/journal.pone.0275364.t001

considered as a fractional derivative when it mandatorily satisfies the criteria formulated by Ortigueira and Machado [56, 57].

2.1.1. Introducing the Caputo fractional operator. The Caputo fractional derivative was selected in the present study because it has been revisited and analyzed under wide sense criterion and strict sense criterion, then fulfilling properties such as linearity, identity, backward compatibility, index law, and generalized Leibniz rule [56, 57]. Additionally, another feature motivating the use of the Caputo operator is related to the differentiation of a constant function, because ${}_{t0}^{C}D_t^q k = 0$ where $k \in \mathbb{R}$. Moreover, unlike fractional differential equations with Riemann-Liouville derivative, which are initialized by derivatives of fractional-order, an initial value problem for fractional differential equations with Caputo's derivatives can be formulated as in ordinary differential equations.

Definition 1 [58]: The Caputo fractional derivative with order $q>1$ for a function $f(t) \in \mathbb{C}^n([t_0,\infty), \mathbb{R})$ is defined

$$ {}_{t0}^{C}D_t^q f(t) = \frac{1}{\Gamma(n-q)} \int_{t_0}^{t} \frac{f^{(n)}(s)}{(t-s)^{q-n+1}} ds \tag{8A} $$

on the interval $[t_0, t]$. When $0<q<1$ is given as follows

$$ {}_{t0}^{C}D_t^q f(t) = \frac{1}{\Gamma(1-q) \int_{t_0}^{t} \frac{f'(s)}{(t-s)^q} ds}. \tag{8B} $$

When $({}_{t_0}^{c}D_t^1 = D$, we recover the standard integer-order derivative whereas ${}_{t0}^{C}D_t^0 = I$ is the identity operator. Using the fractional-order operator of the Caputo derivative in Eq (8), we get the proposed fractional-order socially buffered response model as follows

$$ {}_{t0}^{C}D_t^{q_1} X = k_1 A + (k_2 B - k_6)X + k_3 Y - k_4 XZ - k_5 X^2, \tag{9} $$

$$ {}_{t0}^{C}D_t^{q_2} Y = k_6 X - k_7 Y, \tag{10} $$

$$ {}_{t0}^{C}D_t^{q_3} Z = k_8 (S_0 - Z)Y - \beta k_4 XZ - k_9 Z. \tag{11} $$

Based on the predictor-corrector Adams-Bashforth-Moulton (ABM) integrator, which relies on the analytical property that the initial value problem ${}_{a}D_t^q y(x) = f(x, y(x))$ is equivalent to the Volterra integral [59], we can obtain the discretized form of the system as follows:

$$ X_{n+1}(t) = X_0 + \frac{h^{q_1}}{\Gamma(q_1+2)} (f_1(X_{n+1}^p, Y_{n+1}^p, Z_{n+1}^p) + \sum_{j=0}^{n} \alpha_{1,j,n+1} f_1(X_j, Y_j, Z_j)), \tag{12} $$

$$ Y_{n+1}(t) = Y_0 + \frac{h^{q_2}}{\Gamma(q_2+2)} (f_2(X_{n+1}^p, Y_{n+1}^p, Z_{n+1}^p) + \sum_{j=0}^{n} \alpha_{2,j,n+1} f_2(X_j, Y_j, Z_j)), \tag{13} $$

$$ Z_{n+1}(t) = Z_0 + \frac{h^{q_3}}{\Gamma(q_3+2)} (f_3(X_{n+1}^p, Y_{n+1}^p, Z_{n+1}^p) + \sum_{j=0}^{n} \alpha_{3,j,n+1} f_3(X_j, Y_j, Z_j)), \tag{14} $$

where

$$ X_{n+1}^p(t) = X_0 + \frac{1}{\Gamma(q_1)} \sum_{j=0}^{n} \beta_{1,j,n+1} f_1(X_j, Y_j, Z_j), \tag{15} $$

$$Y_{n+1}^{p}(t) = Y_0 + \frac{1}{\Gamma(q_2)}\sum_{j=0}^{n}\beta_{2,j,n+1}f_2(X_j, Y_j, Z_j), \tag{16}$$

$$Z_{n+1}^{p}(t) = Z_0 + \frac{1}{\Gamma(q_3)}\sum_{j=0}^{n}\beta_{3,j,n+1}f_3(X_j, Y_j, Z_j), \tag{17}$$

with

$$\alpha_{i,j,n+1} = \begin{cases} n^{q_i+1} - (n-q_i)(n+1)^{q_i}, j = 0, & j = 0 \\ (n-j+2)^{q_i+1} + (n-j)^{q_i+1} - 2(n-j+1)^{q+1}, & 1 \le j \le n \\ 1, & j = n+1 \end{cases}$$

and

$$\beta_{i,j,n+1} = \frac{h^{q_i}}{q_i}\left((n+1-j)_i^q - (n-j)_i^q\right).$$

Here, X_0, Y_0, Z_0, are the initial conditions, and f_1, f_2, and f_3 are the right-hand sides of Eqs (5)–(7) as $f_1(X, Y, Z) = k_1A + (k_2B - k_6)X + k_3Y - k_4XZ - k_5X^2$, $f_2(X, Y, Z) = k_6X - k_7Y$, and $f_3(X, Y, Z) = k_8(S_0 - Z)Y - \beta k_4XZ - k_9Z$. If $q_i = q$, for i = 1,2,3, the system is said to be commensurate and the convergence order is described as $|Y(t_n) - Y_n| = \mathcal{O}(h^{\min(2,1+q)}), h \to 0$.

2.2. Equilibrium points of the stationary states

Setting ${}_{t0}^{C}D_t^q = f(X, Y, Z; t) = 0$ in Eqs (9–11) yields the equilibrium points $E_i = (X^*, Y^*, Z^*)$, which are E_1 = (2.58, 2.58,0.90), E_2 = (−0.009, −0.009, −54.8), and E_3 = (−1.31, −1.31,0.91). It can be observed that only the stationary state E_1 has positive values for X, Y, Z. Therefore, it represents an individual's unchanging but dynamic state, i.e., a "dynamic equilibrium". In this case, the stable stationary states can represent regions of generalized homeostasis, where some degree of dynamic constancy exists and can be sustained even under perturbation. By linearizing the system described in Eqs (9–11), we can study the stability of the stationary state E_1 when the parameter B is varied. This parameter is important because it is considered as a psychological variable representing how much stress tends to build more stress. This phenomenon is sometimes referred to as "kindling."

Lemma 1: *The equilibrium point E_1 of the fractional-order socially buffered response model described in Eqs (9–11)* with $B \in [1,2.2]$ and the parameters included in Table 1 is unstable for all $q \in [0, 1)$ [60].

Proof. The characteristic equation of the fractional-order socially buffered response model is described in Eqs (9–11) at equilibrium point (2.58, 2.58,0.90) is given as $\lambda^3+4.016\lambda^2-1.306\lambda+0.033 = 0$. Here, $\lambda_{2,3}$ are positive, real numbers. Therefore, the equilibrium point E_1, considering $B \in [1,2.2]$, is unstable for all $q \in [0, 1]$.

2.3. The chaotic effect of memory in stress-related fractional-order social buffering

Regarding the previously presented integer-order version of the socially buffered response model, we have added the effect of memory in the mathematical model to analyze people's stress-related processes. As well-known, if two Markovian processes (integer-order) start at

two different times, the evolution of both processes is identical. However, the scenario is completely different for a non-Markovian approach (fractional-order), in which the memory plays the main role [61, 62]. In the proposed model, the strength (through the "length") of the memory is controlled by the fractional-order. As q tends to 0, the influence of memory increases and vice-versa. It is important to point out that we only analyze the commensurate case, i.e., all the fractional orders are identical. For the scenario whereby incommensurate orders are needed, the stability analysis in section 2.2 should be derived using Theorem 4.6, page 79, given in [60]. In the commensurate framework, we hypothesize that the perceived psychological stress, $X(t)$, should change as time evolves. For instance, the perceived stress could be lower when a person faces taxing life events at early stages than when he or she is initially stressed. Indeed, the symptoms of stress-related ill-health, $Y(t)$, may get worse due to the accumulative stress effects. Finally, the received social support, $Z(t)$, could reduce the stress impact as time evolves. It means the support has no immediate results, but as the person continues receiving such support (memory), it could be more motivated, and then the stress effects could be reduced.

Within the described context, the parameter of the environmental stress A is represented as a periodic forcing, and chaos behavior can then be founded as a function of the fractional-order. In this case, we set $A = A_0+\rho \sin \omega t$, where $A_0 = 1$, and the parameters ρ and ω are the amplitude and angular frequency of the modulation, respectively. We have conducted several numerical simulations under the external perturbation using the algorithm described in Eqs (12–14). Fig 1A–1D show the bifurcation diagrams for $B = 2.2$, $B = 2.0$, $B = 1.5$, and $B = 1.0$, respectively, and for different values of the fractional-order q. As can be seen, the fractional-order q can be considered as a control parameter for the chaos behavior. Therefore, the stress model can alternate between chaos, periodic oscillations, and stable behaviors as the fractional-order q varies. Fig 1E and 1F present the behavior of the force of the periodic perturbation and its frequency when q = 0.99. In this case, the perturbation frequency ω has a narrow interval for the chaotic oscillations, while the force q may set with different values indicating a low sensitivity regarding chaos generation.

An interesting result was also found when the fractional-order q varies in the range (0.8,1), then originating complex stability regions characterized by multiple alternations between periodic and chaotic oscillations, such as Fig 1G displays. The chaotic and periodic attractors are illustrated in Fig 1H and 1I, when $q = 0.99$ and $q = 0.98$, respectively. The validation of the chaotic oscillations in the fractional-order stress model was performed by the Lyapunov exponent method. For the case of chaotic behavior, the Lyapunov spectrum was LE1 = 0.203, LE2 = 0, and LE3 = −12.707 by applying the Benettin–Wolf algorithm modeled by Caputo's derivative [63]. The Dimension Kaplan-Yorke is DKY = 2.984, which is computed by considering the definition 1 presented in [64]. Finally, the multi-stability in the fractional-order system for different values of arbitrary initial conditions for Y and Z, respectively, was also discovered. This result suggests that stress analyzed with the proposed fractional-order social support buffered response model is affected not only by the system parameters, but also by the initial conditions. More specifically, Fig 1K and 1L show switching between chaos and stable dynamics, thus highlighting that the psychological stress perceived by an individual can be affected by the initial conditions for the symptoms of stress-related ill-health, as well as for the initial conditions of the received social support.

It is worth noting that bifurcation diagrams were also conducted for q in (0,0.8); however, the results are not shown since they tend to either periodic behaviors or unbounded solutions, respectively. In this manner, we focus on the interval $q\in[0.8,1]$ as given in Fig 1(A)–1(D) and Fig 1(G). This finding agrees with the literature on fractional-order systems, where the fractional orders for detecting chaos phenomena are typically $q\geq 0.8$ [65].

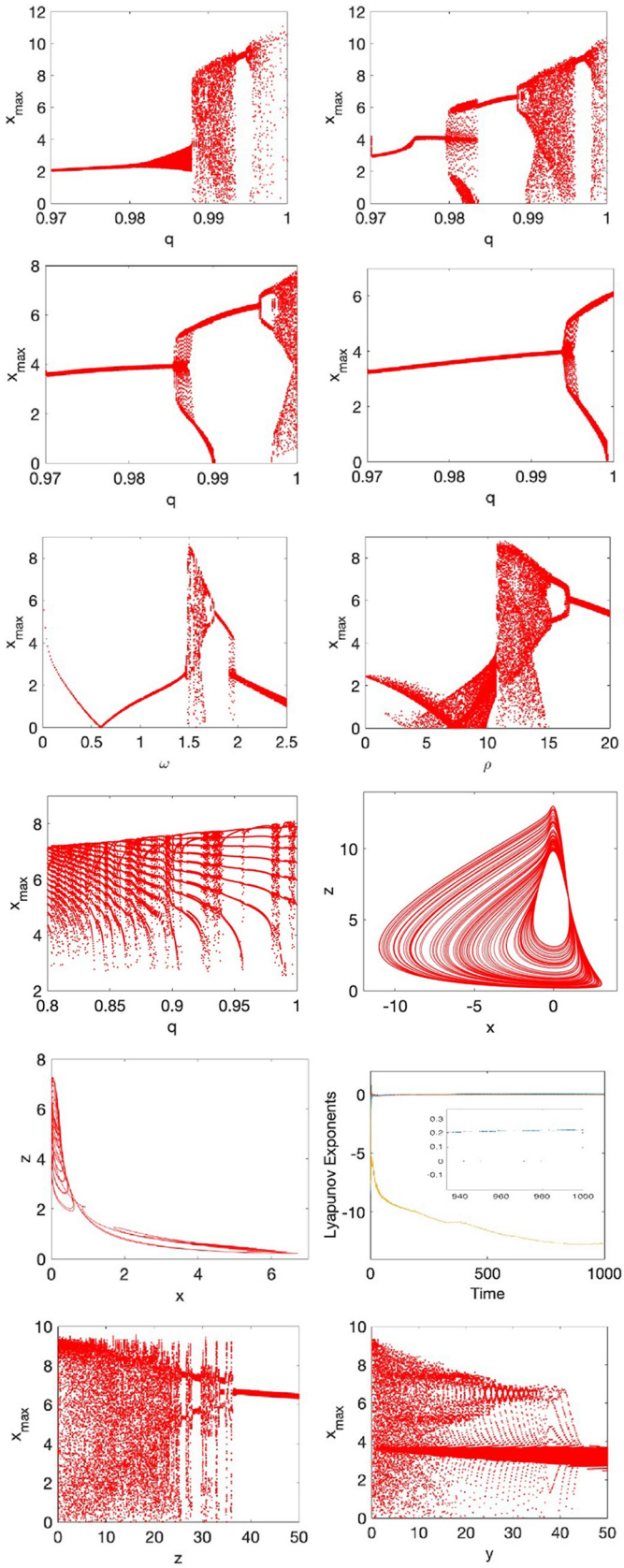
x_max
q
ω
ρ
z
x
Lyapunov Exponents
Time
y

Fig 1. Nonlinear behaviors of the fractional-order stress system. Bifurcation diagrams as a function of the fractional-order q with ρ = 11, ω = 1.5, for a) B = 2.2, b) B = 2.0, c) B = 1.5, and d) B = 1.0. e) Bifurcation diagram for ω with q = 0.99, ρ = 11, and B = 2.2. f) Bifurcation diagram for ρ with q = 0.99, ω = 1.5, and B = 2.2. g) Bifurcation diagram varying q with ρ = 1, B = 2.2 and ω = 0.45. h) Chaotic attractor obtained from parameters in the subfigure a) when q = 0.99. i) Chaotic attractor obtained from parameters in the subfigure a) when q = 0. 98. j) Lyapunov exponents for the chaotic attractor in subfigure h) resulting in LE1 = 0.203, LE2 = 0, LE3 = -12.707 (magnified area from 940s to 1000s). k) and l) k) and l) Bifurcation diagrams showing the switching between chaos and stable dynamics.

https://doi.org/10.1371/journal.pone.0275364.g001

3. Complex nonlinear dynamics

The study of complex systems is often addressed by characterizing their resulting empirical time series in search of patterns and laws that rule their main dynamics. A variety of measures of entropy, relative entropy, complexity, fractal dimensions, etc., have been used for that purpose [66, 67]. In general terms, these metrics can be divided into two groups, i.e., those estimating the global structure of a time series, and those quantifying its time behavior. Whereas the former measure entropy or complexity of a sequence through its spectral distribution, the latter estimate regularity or predictability of a time series by analyzing its time distribution of samples. Although both kinds of indices have reported interesting results in diverse scenarios [68, 69], those based on the spectral transformation of the data provide a global statistical significance and then an easier interpretation. Indeed, these metrics analyze global energy features of a time series without paying special attention to specific local sequences [70]. Two common indices within this group are spectral entropy (SE) and C_0 complexity. Both metrics have been used here to characterize the system described in Eqs (9–11).

From a mathematical point of view, given a time series of N samples in length, i.e., $x(n) = \{x(0), x(1), \ldots, x(N-1)\}$, computation of both SE and C_0 complexity starts by removing its current part, such that

$$x(n) = x(n) - \bar{x}, \tag{18}$$

where $\bar{x} = \frac{1}{N}\sum_{n=0}^{N-1} x(n)$. Then, its Fourier transform is computed as

$$X(k) = \sum_{n=0}^{N-1} x(n) e^{-j\frac{2\pi nk}{N}}, \tag{19}$$

where k = 0, 1,. . .,N–1, and $j = \sqrt{-1}$ is the unit imaginary. Next, for SE estimation, the relative power spectral density of $x(n)$ is obtained as

$$P(k) = \frac{|X(k)|^2}{\sum_{k=0}^{\frac{N}{2}-1} |X(k)|^2}, \tag{20}$$

Consequently, $\sum_{k=0}^{\frac{N}{2}-1} P(k) = 1$. Then, SE is yielded by computing Shannon Entropy from the resulting spectral density [71], i.e.,

$$SE(x, N) = -\frac{1}{\ln\left(\frac{N}{2}\right)} \cdot \sum_{k=0}^{\frac{N}{2}-1} P(k) \cdot \ln(P(k)). \tag{21}$$

It should be noted that SE is normalized by its highest value, i.e. $\ln\left(\frac{N}{2}\right)$, to range from 0 to 1. The metric quantifies the flatness of the frequency spectrum, such that a high value suggests a flat, uniform spectrum with a broad spectral content, and a low value involves a spectrum with all the power condensed into a single frequency bin, i.e., a less complex, more predictable signal [72].

On the other hand, to compute C_0 complexity, $X(k)$ is modified according to a threshold obtained from the mean spectral power of $x(n)$ [73]. More precisely, that threshold is obtained as

$$G_N = \frac{2 \cdot r}{N} \sum_{k=0}^{\frac{N}{2}-1} |X(k)|^2, \tag{22}$$

where r is a control parameter. Then, the spectral distribution of $x(n)$ is redefined as

$$\tilde{X}(k) = \begin{cases} X(k), & \text{if } |X(k)|^2 > G_N, \\ 0, & \text{if } |X(k)|^2 \leq G_N, \end{cases} \tag{23}$$

and the inverse Fourier transform can be used to obtain $\tilde{x}(n)$, i.e.

$$\tilde{x}(n) = \frac{1}{N} \sum_{k=0}^{N-1} \tilde{X}(k)\, e^{j\frac{2\pi nk}{N}}, \tag{24}$$

where $n = 0, 1, \ldots, N-1$. This new time series keeps the regular part of $x(n)$, and then C_0 complexity can be estimated through the ratio between the irregular part of $x(n)$ and the original signal [73], i.e.,

$$C_0(x, r, N) = \frac{\sum_{n=0}^{N-1} |x(n) - \tilde{x}(n)|^2}{\sum_{n=0}^{N-1} |x(n)|^2}. \tag{25}$$

Clearly, the larger the value of C_0, the larger the complexity of $x(n)$ [73].

In the present work, both SE and C_0 have been computed from the variable $x(n)$ obtained for the system described in Eqs (9–11) by considering the conditions analyzed in the previous section. Thus, Fig 2 shows how dynamics change under the perturbation described in Eq (21) with $\omega = 1.5$, $\rho = 11$, and different values of B and fractional orders q. As can be seen, the results presented by both metrics in Fig 2(A)–2(D) agree with those displayed by Fig 1(A)–1(D), thus clearly discerning between stable and chaotic behaviors. In fact, values of SE and C_0 about 0.4 and 0.12 successfully discriminate between both states. Moreover, according to these thresholds, Fig 2(E) and 2(F) only exhibit chaos for a limited region, defined by values of B between 1.5 and 2.3 and fractional orders q between 0.9875 and 1. Nonetheless, it should be noted that the area showing chaos is wider when q increases.

On the other hand, Fig 3 shows the variation of SE and C_0 as a function of both the force (ρ) and the frequency (ω) of the perturbation, when the fractional order q is set to 0.99. As can be seen in Fig 3(A) and 3(B), in both cases, the evolution is consistent with the bifurcation diagrams presented in Fig 1(E) and 1(F). Indeed, when ρ is fixed to 11, chaotic behavior is only noticed when ω ranges from 1.5 to 1.7 (see Fig 3(A)). Similarly, when ω is established to 1.5, stable behavior is observed for most values of ρ, apart from those between 11 and 14 (see Fig 3(B)). According to these findings, Fig 3(C) and 3(D) also display a narrow area where the system exhibits chaotic behavior. This region is roughly delimited by values of ω between 1.28 and 1.65, and values of ρ between 10.5 and 20.

Regarding the different initial conditions tested for Y and Z, values of SE and C_0 displayed by Fig 4(A) and 4(B) were also in agreement with the bifurcation diagrams shown by Fig 1(k) and 1(l), thus presenting a multi-stable behavior of the system. Thus, chaotic behavior is only observed for a narrow range of initial values of Y from 0 to 2.5, approximately. Contrarily, a broader range of initial conditions of Z from 6 to 35 exhibit chaos. According to these results, contour plots of SE and C_0 displayed in Fig 4(C) and 4(D) also present a chaotic region limited by a few initial values of Y (between 0 and 7) and most values of Z (between 0 and 50).

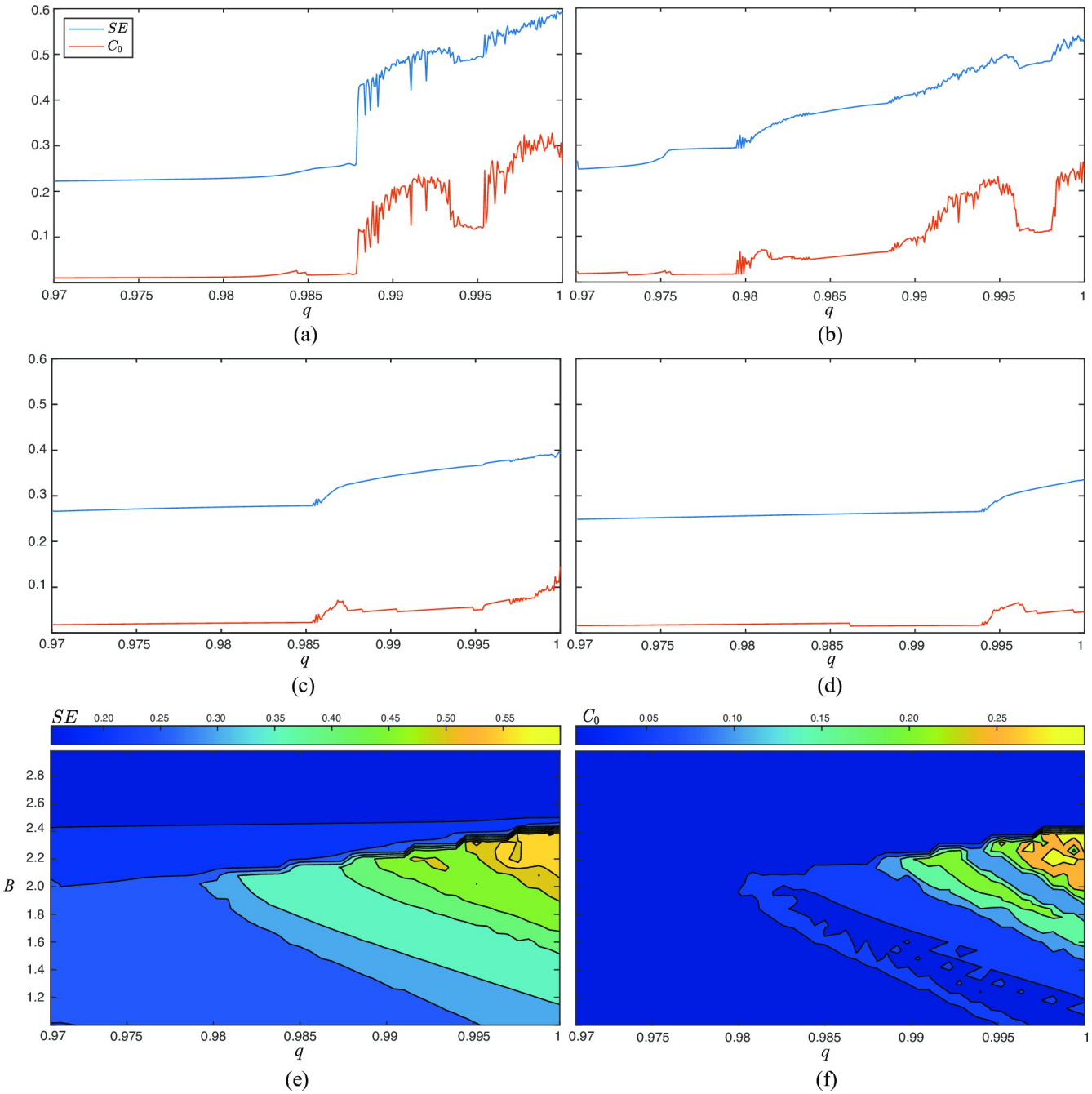

Fig 2. Variation of SE and C_0 as a function of B and q for several scenarios. In all cases, SE and C_0 were computed from the variable $x(n)$ and the parameters $\rho = 11$ and $\omega = 1.5$ were used. In the first four panels the parameter B took values of (a) 2.2, (b) 2.0, (c) 1.5, and (d) 1.0. The two last panels show contour plots for (e) SE, and (f) C_0, when values of B and q range from 1 to 3, and from 0.97 to 1, respectively.

https://doi.org/10.1371/journal.pone.0275364.g002

Nonetheless, it should be noted that the larger the initial value of Z, the wider the region of initial values of Y exhibiting chaos.

Finally, it is worth noting that in all conducted analyses of SE and C_0 have reported similar results. Nonetheless, C_0 has proven to have a slightly higher sensitivity to small changes in the system dynamics, thus better discerning between chaotic and stable behaviors.

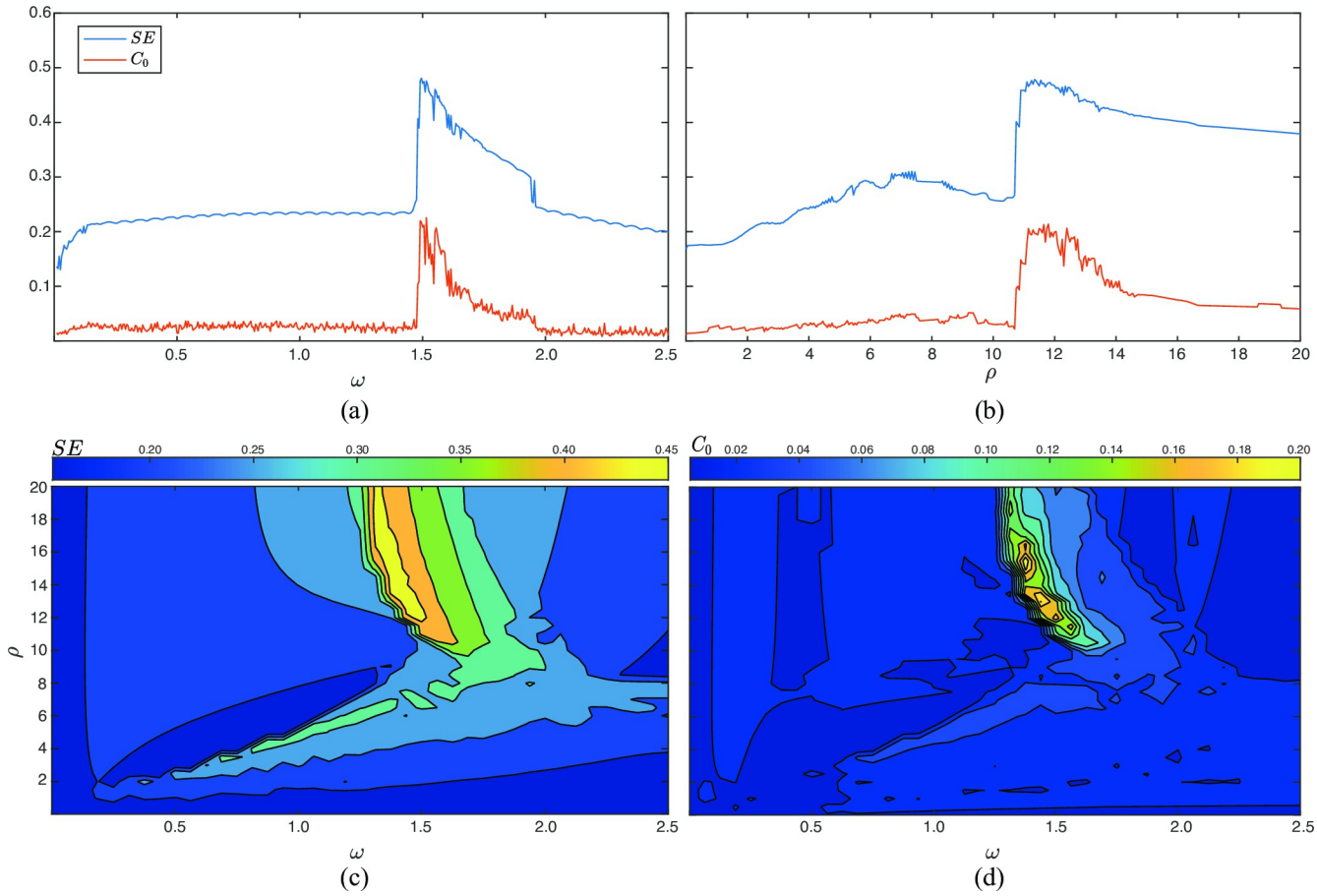

Fig 3. Variation of SE and C_0 as a function of ω and ρ for several scenarios. In all cases, SE and C_0 were computed from the variable $x(n)$ and the parameters $B = 2.2$ and the fractional order $q = 0.99$ were used. In the first two panels the parameters (a) ω and (b) ρ were varied when $\rho = 11$ and $\omega = 1.5$, respectively. The two last panels show contour plots for (c) SE, and (d) C_0, when values of ρ and ω range from 0 to 20, and from 0 to 2.5, respectively.

https://doi.org/10.1371/journal.pone.0275364.g003

4. Conclusions

A fractional-order analysis of a dynamic system modelling people's stress-related processes has been for the first time conducted in the present work. Thus, the stress perceived by an individual under a periodic environmental perturbation has been widely analyzed, and some novel insights have been obtained about how this emotional state relates to external stressors and social support. More precisely, the subject's behavior has proven to be unstable and evolve from a stable stage to chaos for a narrow set of frequency and amplitude values of the external perturbation, when different fractional orders were analyzed. Moreover, our numerical simulations have also conspicuously confirmed that, in some cases, a small deviation in derivative order could result in a completely different dynamical behavior of the system. This finding has been previously unseen since assuming derivative orders to have only integer values restricts simulations and predictions to a limited manner. On the other hand, it has also been shown that not only the system parameters affect stress analyzed with the fractional-order social support buffered response model, but also the initial conditions could considerably affect it. These findings could be helpful in better understanding how an individual reacts to different levels of stressors and social-support recruitment and then taking preventive measures to avoid further health problems. Overall, this study is pioneering research in using fractional calculus for the

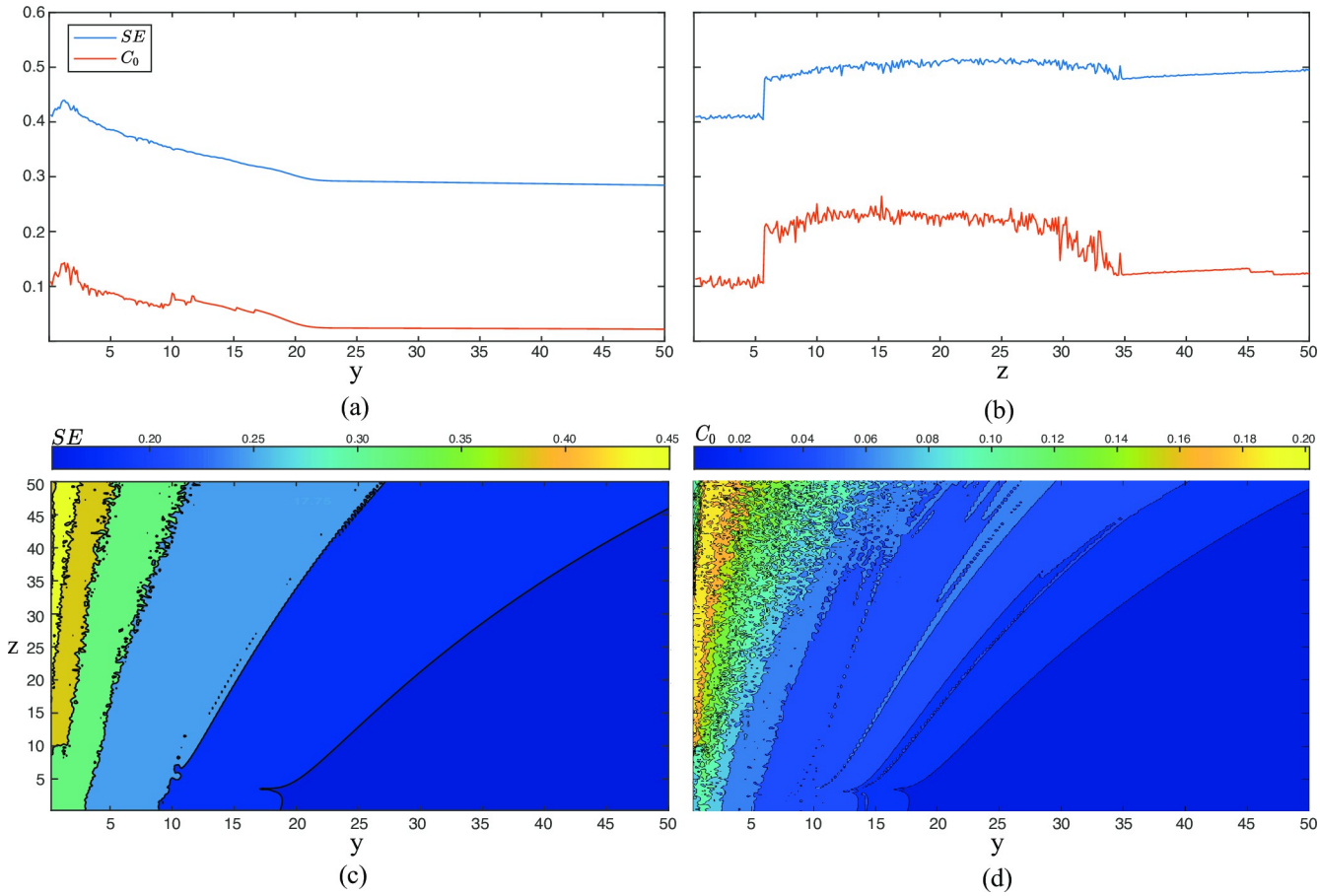

Fig 4. Variation of SE and C_0 as a function of the initial conditions of *y* and *z*. In all cases, SE and C_0 were computed from the variable $x(n)$ and the parameters $q = 0.99$, $\rho = 11$, and $\omega = 1.5$ were used. In the first two panels the values of initial conditions of (a) y and (b) z were ranged from 0 to 50, whereas in the two last panels contour plots for (c) SE, and (d) C_0 are shown.

https://doi.org/10.1371/journal.pone.0275364.g004

analysis of stress, which has demonstrated the importance of considering a fractional framework for such kind of physiological model. As future work, the case where the memory contributions are distinct, i.e., incommensurate fractional orders, could be analyzed.

Author Contributions

Conceptualization: Stelios Bekiros.

Data curation: Hadi Jahanshahi, Jesus M. Munoz-Pacheco.

Formal analysis: Stelios Bekiros.

Investigation: Stelios Bekiros, Hadi Jahanshahi.

Methodology: Stelios Bekiros, Hadi Jahanshahi, Jesus M. Munoz-Pacheco.

Project administration: Stelios Bekiros.

Resources: Stelios Bekiros.

Software: Stelios Bekiros, Hadi Jahanshahi, Jesus M. Munoz-Pacheco.

Supervision: Stelios Bekiros.

Validation: Jesus M. Munoz-Pacheco.

Visualization: Hadi Jahanshahi.

Writing – original draft: Hadi Jahanshahi, Jesus M. Munoz-Pacheco.

Writing – review & editing: Stelios Bekiros.

References

1. Alloway R, Bebbington P. The buffer theory of social support–a review of the literature. Psychological medicine. 1987; 17:91–108. https://doi.org/10.1017/s0033291700013015 PMID: 3575581
2. Cohen S. Stress, social support, and disorder. The meaning and measurement of social support. 1992; 109:124.
3. Praharso NF, Tear MJ, Cruwys T. Stressful life transitions and wellbeing: A comparison of the stress buffering hypothesis and the social identity model of identity change. Psychiatry research. 2017; 247:265–75. https://doi.org/10.1016/j.psychres.2016.11.039 PMID: 27936438
4. Cohen S. Social relationships and health. American psychologist. 2004; 59:676. https://doi.org/10.1037/0003-066X.59.8.676 PMID: 15554821
5. Ganster DC, Victor B. The impact of social support on mental and physical health. British Journal of Medical Psychology. 1988; 61:17–36. https://doi.org/10.1111/j.2044-8341.1988.tb02763.x PMID: 3282536
6. Procidano ME, Fordham U. The nature of perceived social support: Findings of meta-analytic studies. Advances in personality assessment. 1992; 9:1–26.
7. Jahanshahi H, Yousefpour A, Munoz-Pacheco JM, Moroz I, Wei Z, Castillo O. A new multi-stable fractional-order four-dimensional system with self-excited and hidden chaotic attractors: Dynamic analysis and adaptive synchronization using a novel fuzzy adaptive sliding mode control method. Applied Soft Computing. 2020; 87:105943.
8. Jahanshahi H, Yousefpour A, Munoz-Pacheco JM, Kacar S, Pham V-T, Alsaadi FE. A new fractional-order hyperchaotic memristor oscillator: Dynamic analysis, robust adaptive synchronization, and its application to voice encryption. Applied Mathematics and Computation. 2020; 383:125310.
9. Jahanshahi H, Rajagopal K, Akgul A, Sari NN, Namazi H, Jafari S. Complete analysis and engineering applications of a megastable nonlinear oscillator. International Journal of Non-Linear Mechanics. 2018; 107:126–36.
10. Jahanshahi H, Yousefpour A, Wei Z, Alcaraz R, Bekiros S. A financial hyperchaotic system with coexisting attractors: Dynamic investigation, entropy analysis, control and synchronization. Chaos, Solitons & Fractals. 2019; 126:66–77.
11. Jahanshahi H, Munoz-Pacheco JM, Bekiros S, Alotaibi ND. A fractional-order SIRD model with time-dependent memory indexes for encompassing the multi-fractional characteristics of the COVID-19. Chaos, Solitons & Fractals. 2021; 143:110632. https://doi.org/10.1016/j.chaos.2020.110632 PMID: 33519121
12. Sambas A, Vaidyanathan S, Bonny T, Zhang S, Hidayat Y, Gundara G, et al. Mathematical model and FPGA realization of a multi-stable chaotic dynamical system with a closed butterfly-like curve of equilibrium points. Applied Sciences. 2021; 11:788.
13. Sambas A, Vaidyanathan S, Tlelo-Cuautle E, Abd-El-Atty B, Abd El-Latif AA, Guillen-Fernandez O, et al. A 3-D multi-stable system with a peanut-shaped equilibrium curve: Circuit design, FPGA realization, and an application to image encryption. IEEE Access. 2020; 8:137116–32.
14. Mobayen S, Fekih A, Vaidyanathan S, Sambas A. Chameleon chaotic systems with quadratic nonlinearities: An adaptive finite-time sliding mode control approach and circuit simulation. IEEE Access. 2021; 9:64558–73.
15. Musau A. The place of mathematical models in psychology and the social sciences. 2014.
16. Landon AC, Woosnam KM, Boley BB. Modeling the psychological antecedents to tourists' pro-sustainable behaviors: An application of the value-belief-norm model. Journal of sustainable tourism. 2018; 26:957–72.
17. Weger U, Wagemann J. The behavioral, experiential and conceptual dimensions of psychological phenomena: Body, soul and spirit. New Ideas in Psychology. 2015; 39:23–33.
18. Tian X, Jin Y, Chen H, Tang L, Jiménez-Herrera MF. Relationships among social support, coping style, perceived stress, and psychological distress in Chinese lung cancer patients. Asia-Pacific Journal of Oncology Nursing. 2021; 8:172–9. https://doi.org/10.4103/apjon.apjon_59_20 PMID: 33688566

19. Mäntymäki M, Islam AKMN, Turel O, Dhir A. Coping with pandemics using social network sites: A psychological detachment perspective to COVID-19 stressors. Technological Forecasting and Social Change. 2022; 179:121660. https://doi.org/10.1016/j.techfore.2022.121660 PMID: 35400767

20. Zheng K, Chu J, Zhang X, Ding Z, Song Q, Liu Z, et al. Psychological resilience and daily stress mediate the effect of childhood trauma on depression. Child Abuse & Neglect. 2022; 125:105485. https://doi.org/10.1016/j.chiabu.2022.105485 PMID: 35026440

21. Muñoz PT, Franklin TB. The Anxiogenic Effects of Adolescent Psychological Stress in Male and Female Mice. Behavioural Brain Research. 2022:113963. https://doi.org/10.1016/j.bbr.2022.113963 PMID: 35700812

22. Kapasia N, Paul P, Roy A, Das P, Ghosh T, Chouhan P. Perceived academic satisfaction level, psychological stress and academic risk among Indian students amidst COVID-19 pandemic. Heliyon. 2022: e09440. https://doi.org/10.1016/j.heliyon.2022.e09440 PMID: 35600449

23. Chen X, Zou Y, Gao H. Role of neighborhood social support in stress coping and psychological wellbeing during the COVID-19 pandemic: Evidence from Hubei, China. Health & Place. 2021; 69:102532. https://doi.org/10.1016/j.healthplace.2021.102532 PMID: 33752161

24. Cohen S, Wills TA. Stress, social support, and the buffering hypothesis. Psychological bulletin. 1985; 98:310. PMID: 3901065

25. Lo J. Exploring the buffer effect of receiving social support on lonely and emotionally unstable social networking users. Computers in Human Behavior. 2019; 90:103–16.

26. Veiel HOF. Buffer effects and threshold effects: An alternative interpretation of nonlinearities in the relationship between social support, stress, and depression. American Journal of Community Psychology. 1987; 15:717. https://doi.org/10.1007/BF00919800 PMID: 3326409

27. Wang B, Jahanshahi H, Arıcıoğlu B, Boru B, Kacar S, Alotaibi ND. A variable-order fractional neural network: Dynamical properties, Data security application, and synchronization using a novel control algorithm with a finite-time estimator. Journal of the Franklin Institute. 2022.

28. Jahanshahi H, Zambrano-Serrano E, Bekiros S, Wei Z, Volos C, Castillo O, et al. On the dynamical investigation and synchronization of variable-order fractional neural networks: the Hopfield-like neural network model. The European Physical Journal Special Topics. 2022:1–13.

29. Jahanshahi H, Shanazari K, Mesrizadeh M, Soradi-Zeid S, Gómez-Aguilar JF. Numerical analysis of Galerkin meshless method for parabolic equations of tumor angiogenesis problem. The European Physical Journal Plus. 2020; 135:1–23.

30. Jahanshahi H, Chen D, Chu Y-M, Gómez-Aguilar JF, Aly AA. Enhancement of the performance of nonlinear vibration energy harvesters by exploiting secondary resonances in multi-frequency excitations. The European Physical Journal Plus. 2021; 136:1–22.

31. Jahanshahi H, Orozco-López O, Munoz-Pacheco JM, Alotaibi ND, Volos C, Wang Z, et al. Simulation and experimental validation of a non-equilibrium chaotic system. Chaos, Solitons & Fractals. 2021; 143:110539.

32. Delavari H, Heydarinejad H, Baleanu D. Adaptive fractional-order blood glucose regulator based on high-order sliding mode observer. IET Systems Biology. 2018; 13:43–54.

33. Qureshi S, Yusuf A, Shaikh AA, Inc M, Baleanu D. Fractional modeling of blood ethanol concentration system with real data application. Chaos: An Interdisciplinary Journal of Nonlinear Science. 2019; 29:013143. https://doi.org/10.1063/1.5082907 PMID: 30709148

34. Xiong P-Y, Jahanshahi H, Alcaraz R, Chu Y-M, Gómez-Aguilar JF, Alsaadi FE. Spectral entropy analysis and synchronization of a multi-stable fractional-order chaotic system using a novel neural network-based chattering-free sliding mode technique. Chaos, Solitons & Fractals. 2021; 144:110576.

35. Li J-F, Jahanshahi H, Kacar S, Chu Y-M, Gómez-Aguilar JF, Alotaibi ND, et al. On the variable-order fractional memristor oscillator: Data security applications and synchronization using a type-2 fuzzy disturbance observer-based robust control. Chaos, Solitons & Fractals. 2021; 145:110681.

36. Wang Y-L, Jahanshahi H, Bekiros S, Bezzina F, Chu Y-M, Aly AA. Deep recurrent neural networks with finite-time terminal sliding mode control for a chaotic fractional-order financial system with market confidence. Chaos, Solitons & Fractals. 2021; 146:110881.

37. Jahanshahi H, Sajjadi SS, Bekiros S, Aly AA. On the development of variable-order fractional hyperchaotic economic system with a nonlinear model predictive controller. Chaos, Solitons & Fractals. 2021; 144:110698.

38. He Z-Y, Abbes A, Jahanshahi H, Alotaibi ND, Wang Y. Fractional-order discrete-time SIR epidemic model with vaccination: Chaos and complexity. Mathematics. 2022; 10:165.

39. Almalahi MA, Panchal SK, Shatanawi W, Abdo MS, Shah K, Abodayeh K. Analytical study of transmission dynamics of 2019-nCoV pandemic via fractal fractional operator. Results in physics. 2021; 24:104045.

40. Almalahi MA, Panchal SK, Jarad F. Stability results of positive solutions for a system of ψ-Hilfer fractional differential equations. Chaos, Solitons & Fractals. 2021; 147:110931.

41. Abdo MS, Shah K, Wahash HA, Panchal SK. On a comprehensive model of the novel coronavirus (COVID-19) under Mittag-Leffler derivative. Chaos, Solitons & Fractals. 2020; 135:109867. https://doi.org/10.1016/j.chaos.2020.109867 PMID: 32390692

42. Ahmad WM, El-Khazali R. Fractional-order dynamical models of love. Chaos, Solitons & Fractals. 2007; 33:1367–75.

43. Gu R, Xu Y. Chaos in a fractional-order dynamical model of love and its control. Nonlinear Mathematics for Uncertainty and Its Applications: Springer; 2011. p. 349–56.

44. Song L, Xu S, Yang J. Dynamical models of happiness with fractional order. Communications in Nonlinear Science and Numerical Simulation. 2010; 15:616–28.

45. Song L, Yang J. Chaos control and synchronization of dynamical model of happiness with fractional order. IEEE. p. 919–24.

46. Field RJ, Gallas JAC, Schuldberg D. Periodic and chaotic psychological stress variations as predicted by a social support buffered response model. Communications in Nonlinear Science and Numerical Simulation. 2017; 49:135–44.

47. Field RJ, Schuldberg D. Social-support moderated stress: A nonlinear dynamical model and the stress buffering hypothesis. Nonlinear dynamics, psychology, and life sciences. 2011; 15:53. PMID: 21176439

48. Lazarus RS, Folkman S. Stress, appraisal, and coping: Springer publishing company; 1984.

49. DeLongis A, Coyne JC, Dakof G, Folkman S, Lazarus RS. Relationship of daily hassles, uplifts, and major life events to health status. Health psychology. 1982; 1:119.

50. Field RJ, Noyes RM. Oscillations in chemical systems. IV. Limit cycle behavior in a model of a real chemical reaction. The Journal of Chemical Physics. 1974; 60:1877–84.

51. Epstein IR, Pojman JA. An introduction to nonlinear chemical dynamics: oscillations, waves, patterns, and chaos: Oxford University Press; 1998.

52. Cohen JA, Mannarino AP, Kliethermes M, Murray LA. Trauma-focused CBT for youth with complex trauma. Child abuse & neglect. 2012; 36:528–41. https://doi.org/10.1016/j.chiabu.2012.03.007 PMID: 22749612

53. Greeson JK, Briggs EC, Kisiel CL, Layne CM, Ake GS, Ko SJ, et al. Complex trauma and mental health in children and adolescents placed in foster care: Findings from the National Child Traumatic Stress Network. Child welfare. 2011; 90:91–108. PMID: 22533044

54. Zhou P, Ma J, Tang J. Clarify the physical process for fractional dynamical systems. Nonlinear Dynamics. 2020:1–12.

55. Teodoro GS, Machado JAT, De Oliveira EC. A review of definitions of fractional derivatives and other operators. Journal of Computational Physics. 2019; 388:195–208.

56. Ortigueira MD, Machado JAT. What is a fractional derivative? Journal of Computational Physics. 2015; 293:4–13.

57. Ortigueira M, Machado J. Which derivative? Fractal and Fractional. 2017; 1:3.

58. Li C, Deng W. Remarks on fractional derivatives. Applied Mathematics and Computation. 2007; 187:777–84.

59. Diethelm K, Ford NJ, Freed AD. Detailed error analysis for a fractional Adams method. Numerical algorithms. 2004; 36:31–52.

60. Petráš I. Fractional-order nonlinear systems: modeling, analysis and simulation: Springer Science & Business Media; 2011.

61. Ebadi H, Saeedian M, Ausloos M, Jafari GR. Effect of memory in non-Markovian Boolean networks illustrated with a case study: A cell cycling process. EPL (Europhysics Letters). 2016; 116:30004.

62. Van Mieghem P, Van de Bovenkamp R. Non-Markovian infection spread dramatically alters the susceptible-infected-susceptible epidemic threshold in networks. Physical review letters. 2013; 110:108701. https://doi.org/10.1103/PhysRevLett.110.108701 PMID: 23521310

63. Danca M-F, Kuznetsov N. Matlab code for Lyapunov exponents of fractional-order systems. International Journal of Bifurcation and Chaos. 2018; 28:1850067.

64. Zambrano-Serrano E, Anzo-Hernández A. A novel antimonotic hyperjerk system: Analysis, synchronization and circuit design. Physica D: Nonlinear Phenomena. 2021; 424:132927.

65. Tavazoei MS, Haeri M. A necessary condition for double scroll attractor existence in fractional-order systems. Physics Letters A. 2007; 367:102–13.

66. Namdari A, Li Z. A review of entropy measures for uncertainty quantification of stochastic processes. Advances in Mechanical Engineering. 2019; 11:1687814019857350.

67. Ribeiro HV, Jauregui M, Zunino L, Lenzi EK. Characterizing time series via complexity-entropy curves. Physical Review E. 2017; 95:062106. https://doi.org/10.1103/PhysRevE.95.062106 PMID: 28709196

68. Borowska M. Entropy-based algorithms in the analysis of biomedical signals. Studies in Logic, Grammar and Rhetoric. 2015; 43:21–32.

69. Li Y, Wang X, Liu Z, Liang X, Si S. The entropy algorithm and its variants in the fault diagnosis of rotating machinery: A review. IEEE Access. 2018; 6:66723–41.

70. Munoz-Pacheco JM, Zambrano-Serrano E, Volos C, Jafari S, Kengne J, Rajagopal K. A new fractional-order chaotic system with different families of hidden and self-excited attractors. Entropy. 2018; 20:564. https://doi.org/10.3390/e20080564 PMID: 33265653

71. Inouye T, Shinosaki K, Sakamoto H, Toi S, Ukai S, Iyama A, et al. Quantification of EEG irregularity by use of the entropy of the power spectrum. Electroencephalography and clinical neurophysiology. 1991; 79:204–10. https://doi.org/10.1016/0013-4694(91)90138-t PMID: 1714811

72. Sleigh JW, Steyn-Ross DA, Steyn-Ross ML, Grant C, Ludbrook G. Cortical entropy changes with general anaesthesia: theory and experiment. Physiological measurement. 2004; 25:921. https://doi.org/10.1088/0967-3334/25/4/011 PMID: 15382831

73. En-hua S, Zhi-jie C, Fan-ji G. Mathematical foundation of a new complexity measure. Applied Mathematics and Mechanics. 2005; 26:1188–96.